ORIGINAL PAPER



Estimating microbial mat biomass in the McMurdo Dry Valleys, Antarctica using satellite imagery and ground surveys

Sarah N. Power¹ · Mark R. Salvatore² · Eric R. Sokol³ · Lee F. Stanish³ · J. E. Barrett¹

Received: 22 October 2019 / Revised: 23 August 2020 / Accepted: 27 August 2020 / Published online: 18 September 2020 © Springer-Verlag GmbH Germany, part of Springer Nature 2020

Abstract

Cyanobacterial mat communities are the main drivers of primary productivity in the McMurdo Dry Valleys, Antarctica. These microbial communities form laminar mats on desert pavement surfaces adjacent to glacial meltwater streams, ponds, and lakes. The low-density nature of these communities and their patchy distribution make assessments of distribution, biomass, and productivity challenging. We used satellite imagery coupled with in situ surveying, imaging, and sampling to systematically estimate microbial mat biomass in selected wetland regions in Taylor Valley, Antarctica. On January 19th, 2018, the WorldView-2 multispectral satellite acquired an image of our study areas, where we surveyed and sampled seven 100 m^2 plots of microbial mats for percent ground cover, ash-free dry mass (AFDM), and pigment content (chlorophyll-a, carotenoids, and scytonemin). Multispectral analyses revealed spectral signatures consistent with photosynthetic activity (relatively strong reflection at near-infrared wavelengths and relatively strong absorption at visible wavelengths), with average normalized difference vegetation index (NDVI) values of 0.09 to 0.28. Strong correlations of microbial mat ground cover ($R^2 = 0.84$), biomass ($R^2 = 0.74$), chlorophyll-a content ($R^2 = 0.65$), and scytonemin content ($R^2 = 0.98$) with logit transformed NDVI values demonstrate that satellite imagery can detect both the presence of microbial mats and their key biological properties. Using the NDVI—biomass correlation we developed, we estimate carbon (C) stocks of 21,715 kg (14.7 g C m⁻²) in the Canada Glacier Antarctic Specially Protected Area, with an upper and lower limit of 74,871 and 6312 kg of C, respectively.

 $\textbf{Keywords} \ \ Antarctica \cdot Microbial \ mat \cdot Multispectral \ imagery \cdot NDVI \cdot No stocales \cdot Remote \ sensing$

Introduction

Autotrophic microbial communities are essential drivers of primary production in extreme ecosystems, such as hot and cold deserts (Elbert et al. 2012), where species of cyanobacteria, chlorophytes, lichens and mosses form laminar mats or "crusts" with thicknesses ranging from millimeters to several centimeters (Prieto-Barajas et al. 2018). These biological

tosynthesis, nutrient cycling, and soil stabilization (Belnap 2003), which are particularly important in environments that lack vascular plants. The low-density nature of these communities, their patchy distribution, and their ability to survive desiccation make assessments of biomass and productivity challenging, especially in polar deserts. For example, in the McMurdo Dry Valleys, Antarctica (76° 30′–78° 30′ S, 160–164° E), cyanobacterial mats are typically dormant for more than 10 months of the year and are sparsely distributed in terrestrial environments, with the greatest densities occurring on the margins of lakes, ponds, and streams. There are currently no systematic measurements of terrestrial biomass in the McMurdo Dry Valleys that are scalable and provide a record suitable for assessing inter-annual variation in photosynthetically active biomass over broad spatial scales.

soil crusts perform key ecological functions, including pho-

The McMurdo Dry Valleys (MDV) are the largest ice-free area on the Antarctic continent of approximately 4500 km² in Southern Victoria Land (Levy 2013) (Fig. 1). The MDV are one of Earth's coldest, driest deserts with mean annual



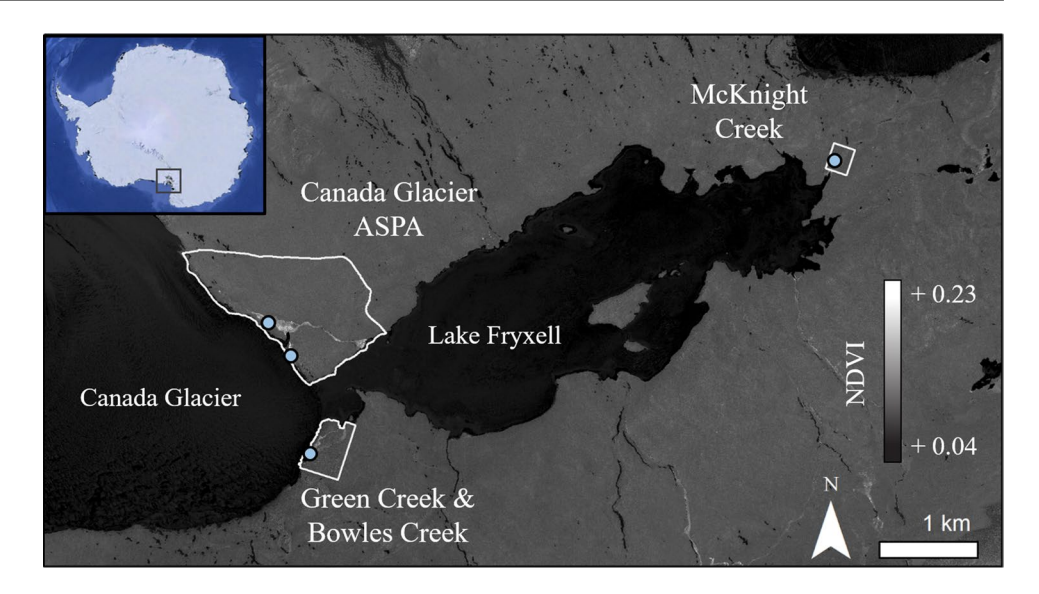
Sarah N. Power snpower@vt.edu

Department of Biological Sciences, Virginia Polytechnic Institute and State University, 2125 Derring Hall, Mail Code 0406, 926 West Campus Drive, Blacksburg, VA 24061, USA

Department of Astronomy & Planetary Science, Northern Arizona University, NAU Box 6010, Flagstaff, AZ 86011, USA

National Ecological Observatory Network, Battelle Memorial Institute, 1685 38th Street, Suite 100, Boulder, CO 80301, USA

Fig. 1 NDVI image of the Fryxell Basin with blue pins denoting the 7 plot locations (Canada Stream, Green Creek, and McKnight Creek) with inset of Antarctica and the McMurdo Dry Valleys shown by gray box. White boundaries denote the carbon extrapolation areas. Image centered at 77.610° S, 163.159° E. Imagery © 2018 DigitalGlobe, Inc.



temperatures between – 15 and – 30 °C and less than 50 mm of precipitation annually (Doran et al. 2002; Fountain et al. 2010). During the austral summers, glacial meltwater feeds streams that flow for up to 10 weeks a year (McKnight et al. 1999). These streams and the sediments and soils around them support diverse microbial communities that persist despite the extreme cold temperatures and short austral summer season. Microbial mat communities form multi-layered sheets in mats in both aquatic and terrestrial environments in the MDV. These microbial mats consist primarily of cyanobacteria (Nostocales and Oscillatoriales), chlorophytes (Prasiola), and bacillariophytes (various diatom species), with filamentous cyanobacteria being the most abundant (Alger et al. 1997). MDV microbial mats can tolerate extreme fluctuations of freeze-thaw and dry-wet cycles (Dodds et al. 1995; Mcknight et al. 2007). They survive winter in a freezedried state and begin photosynthesizing within minutes of thawing and rehydration during the onset of stream flow (Vincent and Howard-Williams 1986; Mcknight et al. 2007).

While the composition and physiology of microbial mats have been studied, current investigation of microbial mat abundance and activity in the MDV is limited to annual surveys of aquatic mats in stream channels and benthic areas of lakes (Hawes et al. 2013; Kohler et al. 2015). Terrestrial mats occurring on the periphery of lake margins and stream riparian zones occupy key transition zones between aquatic habitats and dry mineral soils. Significant nutrient and biotic exchange occur across these ecotones (Ayres et al. 2007; Barrett et al. 2009). Negligible grazing (Treonis et al. 1999), lack of vascular vegetation, and minimal lateral inputs of water or organic material (Gooseff et al. 2011) in the MDV make this stream-soil interface an ideal location to research microbial mat dynamics.

Remote sensing and image analysis can provide longterm, spatially extensive estimates of biomass and primary production and are particularly well suited to the study of remote environments. Remote measurements can be acquired using satellite imagery or unmanned aerial vehicles (UAVs). UAVs have recently proven successful in studying microbial mats and vegetation in the Antarctic (Bollard-Breen et al. 2015; Levy et al. 2020; Miranda et al. 2020). Although UAVs can provide high spatial, spectral, and temporal resolutions, satellites provide synoptic views of landscape-scale ecology without requiring boots on the ground in real time. With method validation, satellite remote sensing will help limit environmental impact on the landscape caused by ecological research in the Antarctic. Remote sensing can be used for the detection of photosynthetic biomass and activity with one such means being the normalized difference vegetation index (NDVI), which evaluates the relationship between reflectance at 680 and 800 nm where photosynthetic materials exhibit a strong diagnostic signal. This signal is primarily caused by chlorophyll-a, which has a unique spectral signature of absorbance in the visible wavelengths and strong reflectance in near-infrared regions due to scattering and reflectance by vegetation cell walls. This marked increase in reflectance, also known as the "red edge" (Collins 1978), is used in spectral analysis as the basis for vegetation indices, such as the NDVI. These indices have been used to derive fundamental vegetation properties, including vegetation biomass, composition, photosynthetic activity, health, identification, and other biophysical and biochemical variables, most notable in forestry and agricultural applications (Mulla 2013; Xue and Su 2017).

NDVI is versatile, designed to broadly identify a variety of photosynthetic species, not just chlorophyll-a. Scytonemin is a cyanobacterial sheath pigment and is commonly found in terrestrial cyanobacteria occupying extreme environments. It is a "microbial sunscreen" as it has an absorption spectrum with a maximum absorbance in the near



ultraviolet, allowing it to screen the cyanobacterial cells from damaging UV radiation (Garcia-Pichel et al. 1992). Scytonemin has been found in cyanobacterial mats, desert biocrusts, and lithic environments (Abed et al. 2010; Vítek et al. 2014), and Vincent et al. (1993) reported extremely high concentrations in the MDV (~10 times that of chlorophyll-a) at Canada Stream. Vincent et al. (1993) found that the microbial mats were stratified with scytonemin and other sheath pigments enriched in upper layers of the mats, while the highest concentrations of chlorophyll-a were found in lower layers. They refer to this area as the "deep Chla maximum" where the chlorophyll-a is most protected from UV radiation by the surface layer of scytonemin and potentially other light-screening pigments (Vincent et al. 1993).

Vegetation indices from remote sensing have been used to measure the dynamics of more inconspicuous vegetation, e.g., microbial mats (Andréfouët et al. 2003). In the Arctic, satellite-derived NDVI has been combined with field survey data to quantify the abundance and biomass of tundra vegetation and mosses (Edwards and Treitz 2017; Hogrefe et al. 2017; Berner et al. 2018). Satellite-derived NDVI has also been applied to vegetation studies in East Antarctica (Jawak et al. 2019) and the Antarctic Peninsula (Fretwell et al. 2011). Although less common, the presence of cyanobacterial soil crusts in arid regions have also been quantified using remote sensing approaches (Karnieli et al. 1999; Rodríguez-Caballero et al. 2017). Salvatore (2015) and Salvatore et al. (2020) demonstrated the utility of remote sensing with microbial mats in the MDV by detecting the spectral signature of chlorophyll-a and their spatial distribution from NDVI using multispectral data from the WorldView-2 satellite (DigitalGlobe, Inc.). Microbial mats inundated by water within the main channels of streams or in lake "moats" do not exhibit as prominent of a spectral signature of chlorophyll due to the absorption of water; however, the terrestrial cyanobacterial mats exhibit strong spectral signatures (Salvatore 2015). Since the MDV is a simple system lacking vascular vegetation, remote sensing is particularly useful here for specific measurements of microbial mats. These remote sensing methods in combination with biological ground surveying have yet to be applied to Antarctic microbial mat communities in the MDV.

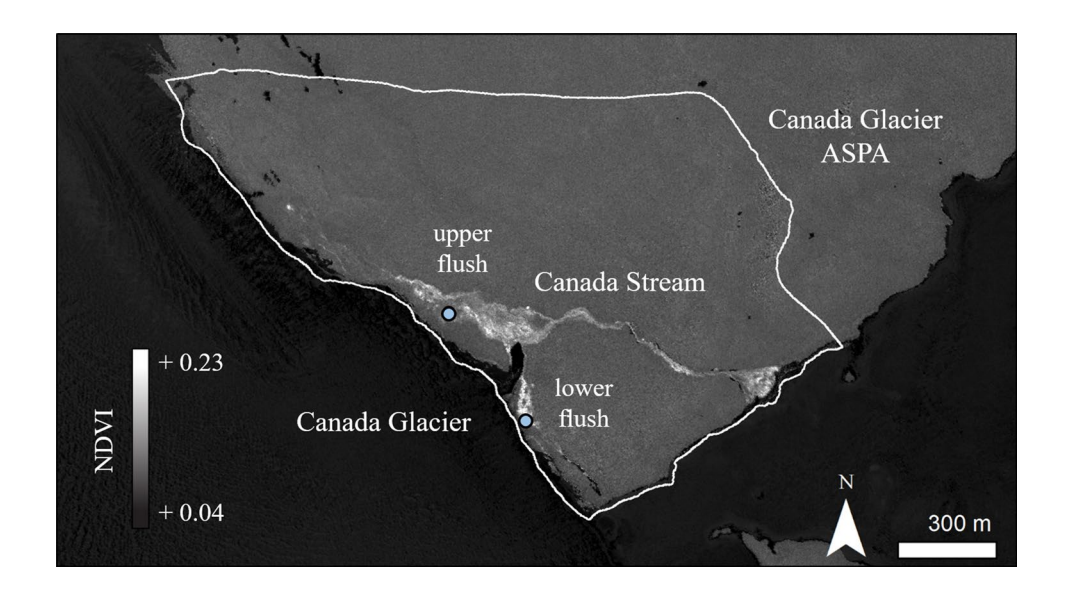
In this study we confirm the utility of multispectral WorldView-2 satellite data in detecting photosynthetic microbial mats in the MDV, and we examine the statistical relationships between NDVI and field-based observations of microbial mat biomass and pigment concentration. To estimate the spatial distribution of terrestrial microbial mats for selected sites in the Lake Fryxell Basin, we: (1) conducted field surveys (i.e., ground cover, ash-free dry mass (AFDM), and pigment content) of microbial mats in a variety of wetlands with high and low visually conspicuous mat cover, (2) processed WorldView-2 multispectral satellite imagery of the Lake Fryxell Basin and derived vegetation indices, and (3) examined correlations of the multispectral data with field survey data. By quantitatively linking field survey data and multispectral satellite data, we developed a statistical model that estimates biomass of microbial mats and moss in the Canada Glacier Antarctic Specially Protected Area (ASPA) (Fig. 2). This estimate represents the first attempt to use remote sensing data to derive such detailed microbial properties and carbon (C) budgets in the McMurdo Dry Valleys.

Methods

Study site

The study sites are located within Taylor Valley, Antarctica where glacier fed streams flow into perennially ice-covered

Fig. 2 NDVI image of the Canada Glacier Antarctic Specially Protected Area (ASPA) outlined in white. The plots are shown in light blue for the upper flush and lower flush sites. Four plots were established adjacent to one another within the lower flush, so they are denoted by a single pin. 21,715 kg of C were estimated in the Canada Glacier ASPA. Image centered at 77.613° S, 163.047° E. Imagery © 2018 DigitalGlobe, Inc.





Lake Fryxell for up to 10 weeks during the austral summer (Fig. 1). The MDV microbial mats are generally described by four characteristic mat types (black, orange, green, and red) based on their appearance, dominant taxa, and habitat preference within the stream (Alger et al. 1997; Kohler et al. 2015). Located within distinct zones based on flow regime and soil/sediment water content, some mats exist mostly in the stream thalweg where flow is most consistent, while the cyanobacterial "black mats" are found along wetted margins not commonly inundated by stream flow where moisture is supplied by the hyporheic zone (Alger et al. 1997; Kohler et al. 2015). These terrestrial microbial mats are dominated by Nostocales. While microbial mat abundance is inherently linked to the availability of water in MDV streams, it is also controlled by geomorphology and characteristics of streambeds, particularly the size and arrangement of streambed cobble and sediments. McKnight et al. (1999) found that microbial mats are most common in medium-gradient streams where the streambed consists of desert pavement with stable cobble composition.

We selected streams that had characteristics suitable for microbial mat growth and known to represent a range in the density of microbial mats that are representative of Taylor Valley (Alger et al. 1997; McKnight et al. 1999). A total of seven 100 m² plots were established, six of which were located on the western side of Lake Fryxell. These plots encompass multiple WV-2 pixels and provide a tractable area for ground-based surveys in the ground time available. Ideally, we would have preferred to sample additional plots spaced further apart; however, our time and mobility in the field were limited. Five of these plots were established beside Canada Stream, which is fed by the Canada Glacier, and are located within the Canada Glacier Antarctic Specially Protected Area (Fig. 2). The ASPA was designated by the Antarctic Treaty System in 2002 as a significant biologically active area of great scientific value as one of the most productive and biologically diverse areas in the MDV. Glacial melt flows over a gently sloping area of approximately 100–200 m² before entering the Canada Stream channel; melt from the northern end forms small channels before flowing into the main stream channel, while melt from the

southern end drains into a pond before entering the main channel (Conovitz et al. 1998). One plot was established in the wetted area north of the pond referred to as "the upper flush" and four others were established in the wetted area south of the pond, "the lower flush" (sensu Schwarz et al. 1992), which are both biologically rich with abundant cyanobacteria, algae, and moss. On the southwestern side of Lake Fryxell, one plot was established at Green Creek, which is also fed by the Canada Glacier and located adjacent to Bowles Creek (Fig. 1). The plot was positioned downstream of a melt pond beside the glacier in a shallow gradient area with visible microbial mat cover. An additional plot was established on the eastern side of Lake Fryxell beside McKnight Creek (Fig. 1), which is fed by the Commonwealth Glacier. Compared to the six other plot locations at Canada Stream and Green Creek, the McKnight Creek plot is much further downstream from its source glacier and has a less stable, sandier substrate, poorly developed desert pavement, and patchier, less abundant microbial mats. Plot locations among each of the streams were selected in areas that were not inundated by water to ensure that the spectral signatures were not dominated by water absorption signatures. Indeed, by avoiding standing water, the microbial mat type present is primarily a black mat and moss mixture, since these vegetation types are most commonly found in wet, not inundated, areas. Other microbial mat types (e.g., orange, red, and green mats) are typically found in the stream thalweg and are therefore less detectable in orbital spectral data using current methods.

Field surveys

Locations of visually conspicuous microbial mats outside of stream channels were selected for plots beside Canada Stream, Green Creek, and McKnight Creek (Table 1). On January 9th and 10th 2018, four 100 m² plots (Canada Stream-1, Canada Stream-2, Canada Stream-3, and Canada Stream-4) were established adjacent to one another in the most productive area of the Canada Stream ASPA, the lower flush (Schwarz et al. 1992), using a tape measure. In the upper flush of the Canada Stream ASPA, a fifth 100

Table 1 Plot locations, including a qualitative comparison of their visual microbial mat abundance and stream area stability

Plot location	Latitude	Longitude	Visual mat abundance	Stream stability
Canada Stream-1	-77° 36′ 58.12″	163° 2′ 27.92″	High	Moderate-gradient, stone pavement
Canada Stream-2	-77° 36′ 57.92″	163° 2′ 29.10″	High	Moderate-gradient, stone pavement
Canada Stream-3	-77° 36′ 58.37″	163° 2′ 28.85″	High	Moderate-gradient, stone pavement
Canada Stream-4	-77° 36′ 58.17″	163° 2′ 30.03″	High	Moderate-gradient, stone pavement
Canada Stream-5	-77° 36′ 47.76″	163° 1′ 52.54″	High	Moderate-gradient, stone pavement
Green Creek	-77° 37′ 30.29″	163° 3′ 0.62″	Moderate	Shallow-gradient, stone pavement
McKnight Creek	-77° 35′ 50.99″	163° 16′ 10.15″	Low	Shallow-gradient, sandy



m² plot (Canada Stream-5) was established on January 11th, 2018. Two additional 100 m² plots were established beside McKnight Creek and Green Creek on January 12th and 25th, 2018, respectively. These plots were selected to encompass a range of low (but apparent) to high microbial mat density based upon previous studies and visual assessment (Alger et al. 1997; McKnight et al. 1999).

Hemispherical photos of ground cover along with position data were taken every 5 m at each of the seven plots from standard heights. The plot locations were marked using a high precision global navigation satellite system (GNSS) receiver (Septentrio ALTUS APS3G) which communicated with a GNSS reference receiver (Trimble NetR8) located at the Lake Fryxell Camp. The receiver unit used real time kinematic (RTK) positioning to gather locations with centimeter level accuracy. The hemispherical photos taken in the field were analyzed for microbial mat cover using ImageJ version 1.51 (U.S. National Institutes of Health), an image analysis software. By converting the photos to binary black and white images, the software distinguished pixels representing microbial mats (black) from those representing bare soil or rocks (white). Each pixel was then classified as either white or black, and an estimate for percent cover was quantified using a histogram.

Using a random stratified sampling design, we surveyed and sampled 2-1 m² subplots within each of the first four Canada Stream plots, with location of subplots depending on the distribution of standing water in the plot. Five locations were selected in each subplot using randomly generated cartesian coordinates for sample collection and point intercept surveys of ground cover and hydrological status. Samples from each subplot were composited for a total of 10 samples from each 100 m² plot. The Canada Stream-5, McKnight Creek, and Green Creek plots were surveyed and sampled at 9 locations every 5 m apart. At each of the sampling points within the 7 plots, we visually assessed the hydrologic status (i.e., inundated, saturated, wet or dry) and the ground cover type (e.g., soil, black mat, green moss, etc.). Microbial mats were each collected in 60 mL amber Nalgene bottles at the 9-10 sample points in each plot. Indeed, the microbial mat samples were commonly a mixture of microbial mat and moss, and these vegetation types were not separated during sampling or lab analyses. Using the current available data, the spectral contributions of microbial mat and moss could not be distinguished, so the combined influence is what we are able to detect and record. The top layer of soil (i.e., ~ 1 cm) was collected for the areas that did not have visible mat cover, following the methods described in Barrett et al. (2004). All soil and mat samples were frozen at – 20 °C until processing and analysis.

Laboratory analysis

The microbial mat samples were stored at -20 °C in the Crary Laboratory in McMurdo Station and then shipped to Virginia Tech in February 2018 for analysis. Chlorophyll-a concentration was measured on the microbial mat samples with a spectrophotometer (Shimadzu UV-1601) using a protocol that corrects for scytonemin concentration, a UVscreening sheath pigment previously reported for this area (Vincent et al. 1993). Throughout the process, care was taken to avoid exposing the samples to light as chlorophylla degrades with exposure to light. The samples were dried at 105 °C for 24 h and extracted in 10 mL of 90% unbuffered acetone using 0.5 g of mat, based on protocols from Garcia-Pichel and Castenholz (1991) and MCM LTER standard methods. The samples were then left for 24 h in a dark room at ambient temperature for complete chlorophyll extraction. After centrifuging for 10 min at 4000 RPM, they were analyzed on a spectrophotometer using 10 mL cuvettes. The absorbances contributed by chlorophyll-a, carotenoids, and scytonemin were quantified at 663, 490, and 384 nm, respectively, using the trichromatic equations outlined in Garcia-Pichel and Castenholz (1991). The pigment concentrations were then quantified using the Beer-Lambert Law with the extinction coefficients also outlined in Garcia-Pichel and Castenholz (1991).

The microbial mat samples were measured for AFDM by weighing approximately 0.25 g of oven-dried sample, combusting at 550 °C for 60 min using a muffle furnace, and reweighing after cooling in a desiccator. Given the extremely low clay content of soils in this region (Barrett et al. 2006a), the rehydration of clays was assumed negligible, so the methods did not include rewetting samples to account for the hydration of clays. Microbial mat biomass (mg organic matter (OM) cm⁻²) was estimated from AFDM (mg g⁻¹) using dry mass per unit area measurements made at each site with a 2.27 cm² coring device. Similarly, pigment concentrations were also expressed on an areal basis (µg cm⁻²) using dry mass per unit area measurements. To correlate spatially with NDVI, biomass and pigment concentrations were scaled by percent cover estimated from the hemispherical photos. The plot-scale biomass was then converted to biomass in g C m⁻² by assuming organic matter is 53% C by weight (Wetzel 1983).

Satellite imagery collection and analysis

WorldView-2 multispectral satellite (DigitalGlobe, Inc.) collected images of the Lake Fryxell Basin during January 2018 to coincide with the timing of field surveys and sample collection. While multiple images were acquired during this time, only one image was cloud-free on January 19, 2018, occurring within 10 days of when we surveyed and



sampled. This WV-2 image was acquired at spatial resolutions of 2.44 m for multispectral bands and 0.62 m for the panchromatic band at 29.3° off-nadir and 19.1° solar elevation. The image was georeferenced using ground-control points and then obtained from the University of Minnesota's Polar Geospatial Center (PGC) through a cooperative agreement between the NSF and National Geospatial-Intelligence Agency (NGA). The image was subsequently processed to atmospherically corrected surface reflectance using the dark object subtraction-regression (DOS-R) method in Salvatore et al. (2014) and Salvatore (2015) using the Environment for Visualizing Images software (ENVI, Harris Geospatial). We then calculated the common NDVI parameter in ENVI, which is a common vegetation index used for determining whether an image contains photosynthesizing vegetation (Tucker 1979). NDVI was calculated as:

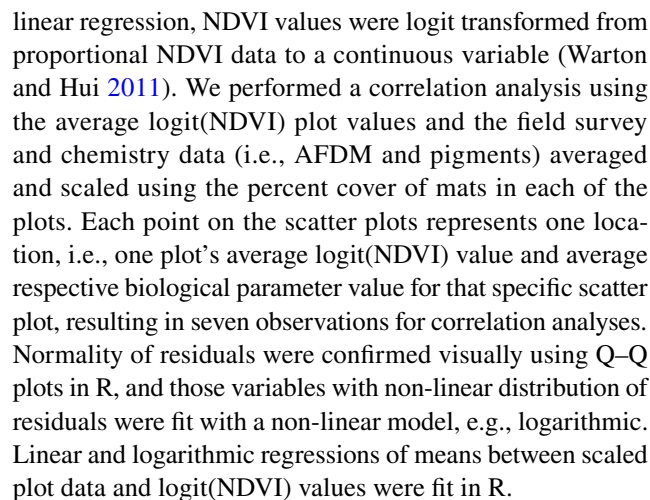
$$\text{NDVI} = \frac{\rho_{\text{NIR}} - \rho_{\text{Red}}}{\rho_{\text{NIR}} + \rho_{\text{Red}}}$$

where $\rho_{\rm NIR}$ and $\rho_{\rm Red}$ represent the spectral reflectance measurements acquired in the near-infrared (770–895 nm, band 7) and red (630–690 nm, band 5) regions, respectively.

To identify the plot locations on the NDVI product image, we re-projected the plot coordinates shapefile from GCS WGS 1984 to Polar Stereographic using ArcMap version 10.5.1 (ESRI) to match the coordinate system of the satellite image. Using ArcMap, we converted the image raster file to points and then selected the pixels whose centroids fell within the 100 m² plot boundaries. The pixels within the plots and beside the edges are a mixture of microbial mat, moss, and soil; therefore, they are not pure mat endmembers. The georeferencing of images can be off by a pixel or two in any direction, depending on the distance from groundcontrol points, and as a result, this pixel-selection method is a way to approximate the plot locations. Each plot corresponds to approximately 14–17 pixels (5.95 m² per pixel) with unique NDVI values. NDVI values of each selected pixel were exported and averaged by plot to compare to the survey and chemistry data.

Statistical analysis

Using R Statistical Software version 3.4.1 (R Core Team 2017), we visualized the field survey, chemistry, and NDVI data with box plots for each of the seven plots to examine the variation within and among plots. After confirming normality using Q–Q plots, we performed one-way analysis of variance (ANOVA) tests on each data set to determine whether the means were statistically different among plots, and Tukey's Honest Significant Difference (TukeyHSD) tests were performed to determine which plots were statistically different from one another. To meet the assumptions for



To extrapolate microbial mat biomass (g C m⁻²) from the Canada Stream, Green Creek and Bowles Creek wetland area, and a portion of the lower reach of McKnight Creek, boundaries were defined in ENVI. The Canada Glacier ASPA boundaries were used to define the area (1.47 km²) for our Canada Stream extrapolations (Fig. 2), while the Green Creek and Bowles Creek wetland area (199,100 m²) was defined based upon using the Canada Glacier and Lake Fryxell margin as boundaries (Fig. 1). The delta of McKnight Creek had noticeably higher NDVI values, due to the proximity of Lake Fryxell and moat/lake microbial mats. Since this area is not comparable to the unstable, lower coverage substrate typical of McKnight Creek, the boundary was defined as the lower reach of McKnight Creek excluding the edge of the lake (58,290 m²) (Fig. 1). NDVI values were then extracted from these areas in ENVI and logit transformed. The linear relationship between logit(NDVI) and the natural logarithm of plot-scale biomass (g C m⁻²) was applied to NDVI values > 0.09 (a vegetation threshold selected based on the average NDVI of our lowest coverage site, Green Creek). Biomass was quantified per pixel (5.95 m²) and then summed together for a total biomass inventory in kg of C at each of the sites. The total biomass was then divided by the total vegetated area (pixels with NDVI > 0.09) to calculate the average areal biomass (g C m⁻²) at each of the three sites. For the Canada Glacier ASPA, a 95% prediction interval was used to calculate an upper and lower biomass estimate in R.

Results

Field survey data

There was high density of microbial mat cover and organic matter content among all plots relative to typical dry soil surfaces (e.g., Burkins et al. 2000; Barrett et al. 2006b). Black mat, which we report as Nostocales, was the majority



of this cover, representing > 85% of microbial mat present in our ground surveys, and the remaining represented by mixed moss, likely Bryum (Schwarz et al. 1992), and epiphytic communities of Nostocales. Plots were selected outside the main channels or thalwegs, and less than 25% of plot sampling areas were inundated, i.e., standing water, though a majority were near saturation. In the Canada Stream plots, 63% were wet to saturated with the remaining portion inundated with standing water. Percent microbial mat cover ranged from 33 to 85%, with the highest coverage in the Canada Stream flush areas and the lowest at the Green Creek and McKnight plots (ANOVA, df = 6, F = 14.31, p < 0.0001) (Table 2, Fig. 3a). Organic matter content ranged from 6.53 to 399 mg AFDM g⁻¹ (Fig. 3b), with dry mass of Nostocales and mixed moss and Nostocales mats of 0.64 to 0.81 g cm⁻² (n = 31, standard deviations of 0.409, 0.717, and 0.469 g cm⁻² for Canada, Green, and McKnight, respectively). The Canada Stream plots had the overall highest biomass of microbial mats averaging 231–711 g C m⁻², while Green Creek and McKnight Creek had the lowest microbial mat biomass with averages of 69 ± 52 g C m⁻² and 144 ± 113 g C m⁻², respectively (Table 3).

Chlorophyll-a, scytonemin, and carotenoid concentrations varied significantly among the seven study plots (ANOVA, df = 6, F = 4.35, p = 0.001; F = 5.04, p = 0.0003; F = 5.01, p = 0.0003, respectively) (Table 2): chlorophyll-a concentration ranged from 0.61 to 48.52 μ g g $^{-1}$, scytonemin concentration ranged from 9.39 to 1163 μ g g $^{-1}$, and carotenoid concentration ranged from 0.25 to 119.9 μ g g $^{-1}$ (Fig. 4). McKnight Creek had the greatest average chlorophyll-a concentration of 24.44 μ g g $^{-1}$, surpassing even the high-density Canada Stream plots (Fig. 4a). Scytonemin concentrations were over an order of magnitude greater than the other pigment concentrations and highly variable, especially in the Canada Stream lower flush plots where scytonemin concentrations were highest (averaging 494.7–700.3 μ g g $^{-1}$)

Table 2 Degrees of freedom, *F*-values, and *p*-values from one-way analysis of variance (ANOVA) tests and plot comparisons of Tukey's honest significant difference (TukeyHSD) tests of percent cover, ashfree dry mass (AFDM), chlorophyll-a, scytonemin, carotenoid, and NDVI data, where "CAN" refers to Canada Stream, "GRN" Green Creek, and "MCK" McKnight Creek

	ANOVA			TukeyHSD ($p < 0.05$)		
	\overline{df}	F	p	Plot comparison		
Percent cover	6	14.31	< 0.0001	CAN 1–5>GRN, MCK		
AFDM	6	4.14	0.00166	CAN 2>GRN, MCK		
Chlorophyll-a	6	4.35	0.00109	MCK>CAN 5, GRN		
Scytonemin	6	5.04	0.00032	CAN 2-4 > GRN		
Carotenoid	6	5.01	0.00034	CAN 2-4 > GRN		
NDVI	6	70.01	< 0.0001	CAN 1–4 > GRN, MCK and CAN 5 > GRN		

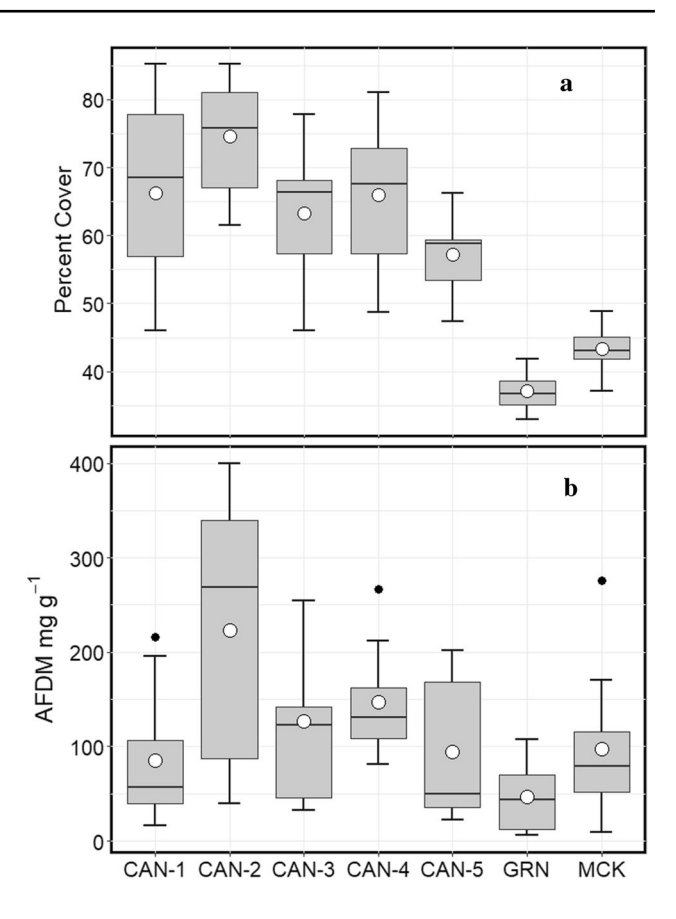


Fig. 3 Microbial mat percent cover (a) and ash-free dry mass (AFDM) from the Canada Stream, Green Creek, and McKnight Creek plots (b). White circles indicate the averages per plot, the horizontal lines indicate the median, and the black circles indicate outliers defined by>1.5×interquartile range (IQR). The whiskers represent the largest value within 1.5×IQR above the 75th percentile and the smallest value within 1.5×IQR below the 25th percentile. "CAN" refers to Canada Stream, "GRN" Green Creek, and "MCK" McKnight Creek

(Fig. 4b). One sample from Canada Stream-2 had extremely high pigment concentrations overall, with values greater than 6 standard deviations of the mean chlorophyll-a concentrations for all observations. Although this data point is not believed to be instrumental error, we removed it from the pigment box plots and the correlation analyses, because it was so far outside the centroid of the distribution and skewed all analyses.

Normalized difference vegetation index relationships

NDVI values extracted from the image at pixels corresponding to our plots ranged from 0.0719 to 0.365 with the highest values and the most variability evident in Canada Stream plots 1–4 (Fig. 5). Although the McKnight Creek plot had the highest average chlorophyll-a concentration, it had the second to lowest average NDVI value, 0.0964. Overall, the



Table 3 Biomass in mg organic matter (OM) cm⁻² and chlorophyll-a (Chl-a) and scytonemin (Scyto) in μg cm⁻² shown for the Canada Stream, Green Creek, and McKnight Creek plots expressed on an areal basis using dry mass per unit area measurements. Data shown were then scaled by percent cover to correlate spatially with NDVI

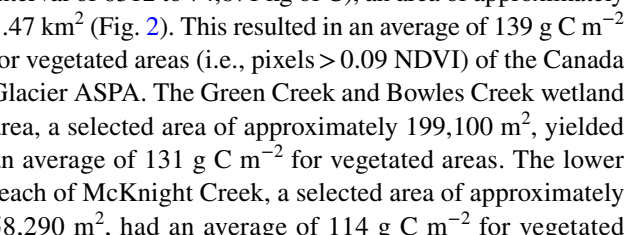
	Dry mass (g cm ⁻²)	% cover	Biomass (mg OM cm ⁻²)	Chl-a (μg cm ⁻²)	Scyto (µg cm ⁻²)	Scaled by % cover		
						Biomass (g C m ⁻²)	Chl-a (g m ⁻²)	Scyto (g m ⁻²)
Canada Stream-1	0.81	66	69	10.8	400	242	0.071	2.65
Canada Stream-2	0.81	75	180	17.4	447	711	0.129	3.33
Canada Stream-3	0.81	63	102	16.6	566	342	0.105	3.58
Canada Stream-4	0.81	66	119	13.9	500	414	0.092	3.30
Canada Stream-5	0.81	57	76	6.1	252	231	0.035	1.45
Green Creek	0.75	37	35	5.6	144	69	0.021	0.53
McKnight Creek	0.64	43	63	15.7	232	144	0.068	1.00

most productive sites (i.e., Canada Stream) were the most variable in terms of AFDM, pigment concentration, and NDVI indices, but also had the highest percent cover of microbial mats (Figs. 3b, 4, 5).

Each of the biological parameters were significantly correlated to the multispectral data. Percent cover was significantly correlated to logit(NDVI) ($R^2 = 0.84$, p = 0.004, logi $t(NDVI) = 0.0169 \times cover - 1.66$), and plot-scale microbial mat biomass in g of C m⁻² had a significant logarithmic relationship with logit(NDVI) ($R^2 = 0.74$, p = 0.013, logit $(NDVI) = 0.283 \times ln(biomass) - 2.24)$ (Fig. 6). Plot-scale chlorophyll-a was significantly correlated to logit(NDVI) $(R^2 = 0.65, p = 0.028, logit(NDVI) = 5.26 \times chloro$ phyll - 1.07), and plot-scale scytonemin had the most significant relationship with logit(NDVI) ($R^2 = 0.98$, p < 0.0001, $logit(NDVI) = 0.197 \times scytonemin - 1.12)$ (Fig. 7).

Upscaling

Using the observed relationship between biomass and NDVI, we extrapolated microbial mat biomass from NDVI to our respective study areas using the following equation: ln(bi omass) = $2.61 \times logit(NDVI) + 7.28 (R^2 = 0.74, p = 0.013)$ (Fig. 8). This equation was only applied to pixels with NDVI values > 0.09, a vegetation threshold selected based on the average NDVI of our lowest coverage site. We estimated 21,715 kg of C in the Canada Glacier ASPA (95% prediction interval of 6312 to 74,871 kg of C), an area of approximately 1.47 km² (Fig. 2). This resulted in an average of 139 g C m⁻² for vegetated areas (i.e., pixels > 0.09 NDVI) of the Canada Glacier ASPA. The Green Creek and Bowles Creek wetland area, a selected area of approximately 199,100 m², yielded an average of 131 g C m⁻² for vegetated areas. The lower reach of McKnight Creek, a selected area of approximately 58,290 m², had an average of 114 g C m⁻² for vegetated areas.





Discussion

Dense microbial mat communities are visible using NDVI in satellite imagery of Taylor Valley, Antarctica. Above ~ 50% ground cover of microbial mat communities in the vicinity of Canada Stream returned NDVI values above 0.1, a value often used as a heuristic cutoff between barren areas and active vegetation. Though, the detection of microbial mats is not anticipated to be comparable to typical uses of NDVI vegetation detection of vascular vegetation, e.g., trees, crops, etc. At the plot level, we have demonstrated that NDVI values are significantly correlated to in situ biological parameters of microbial mats in glacial wetland areas, especially the microbial sunscreen pigment scytonemin. Using these strong correlations, we have extrapolated significant carbon stocks in stream margins, glacial wetland areas, and even outside of stream channels in drier soils, and here we present the first inventory estimate of C content in the Canada Glacier ASPA using satellite imagery.

Microbial mat abundance

Our results show high coverage of microbial mats in the Canada Stream flush areas (averaging 57-75% cover), agreeing with previous studies by Schwarz et al. (1992) and Alger et al. (1997) (Fig. 3a). The plot location at McKnight Creek had a low to moderate cover of microbial mat, 43%, while the plot at Green Creek had the lowest cover, 37% (Fig. 3a). McKnight et al. (1999) found that streams with stable, welldeveloped desert pavement, e.g., Canada Stream and Green Creek, hosted the densest mats in Taylor Valley. In our study, McKnight Creek represents the low end of this spectrum, with unconsolidated course-grained sediments constituting the majority of the plot surface. Previous studies have reported high density of microbial mats within the thalweg and wetted stream margins at Green Creek (Alger et al.

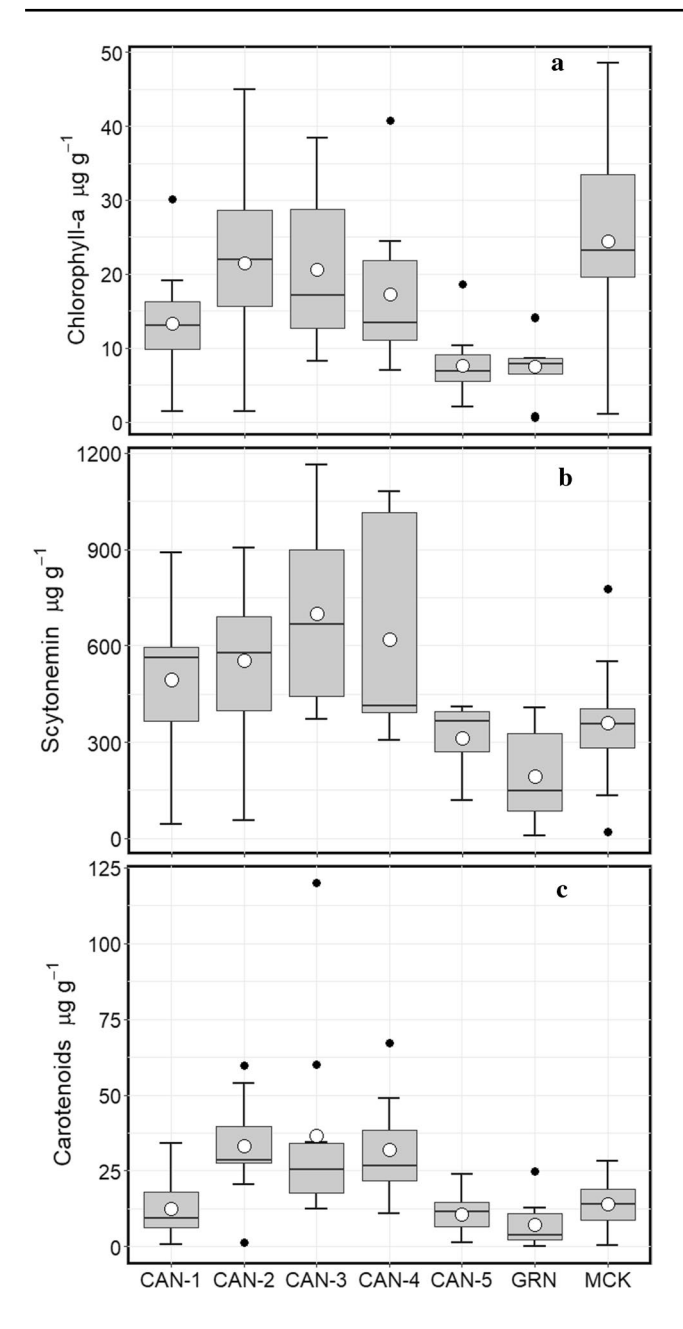


Fig. 4 Chlorophyll-a (**a**), scytonemin (**b**), and carotenoid (**c**) content from the Canada Stream, Green Creek, and McKnight Creek plots. White circles indicate the averages per plot, the horizontal lines indicate the median, and the black circles indicate outliers defined by > 1.5 × interquartile range (IQR). The whiskers represent the largest value within 1.5 × IQR above the 75th percentile and the smallest value within 1.5 × IQR below the 25th percentile. "CAN" refers to Canada Stream, "GRN" Green Creek, and "MCK" McKnight Creek. One outlier sample from Canada Stream-2 was 6, 3, and 4 standard deviations away from the mean chlorophyll-a, scytonemin, and carotenoid data, respectively, and was not included in the box plots or correlation analyses

1997); however, the area we selected to establish the plot was on the stream margins where mats were not as abundant. This was to avoid surveying inundated areas, since currently

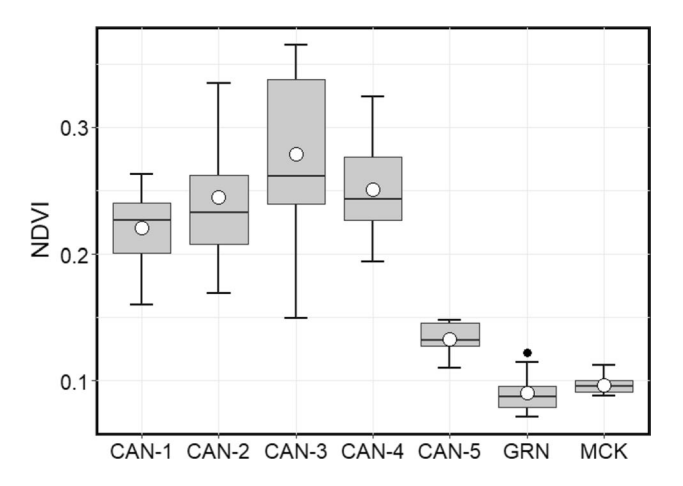


Fig. 5 Box plots illustrating NDVI values from the Canada Stream, Green Creek, and McKnight Creek plots. White circles indicate the NDVI averages per plot, the horizontal lines indicate the median, and the black circles indicate outliers defined by > 1.5 × interquartile range (IQR). The whiskers represent the largest value within 1.5 × IQR above the 75th percentile and the smallest value within 1.5 × IQR below the 25th percentile. "CAN" refers to Canada Stream, "GRN" Green Creek, and "MCK" McKnight Creek

there is little information regarding how water depth affects microbial mat spectral signatures.

There are few scalable estimates of organic matter from the MDV literature for microbial mat biomass, but a previous vegetation study of the Canada Glacier flush areas where mixed moss and microbial mats occur reported biomass values of 95-125 mg OM cm⁻² (Schwarz et al. 1992). Our plot-scale biomass estimates for the Canada Glacier flush, 231–711 g C m⁻², correspond to unscaled biomass estimates of 69-180 mg OM cm⁻², which are comparable to those reported by Schwarz et al. (1992). The range of microbial biomass that we found of 69 g C m⁻² at Green Creek to 711 g C m⁻² at Canada Stream bracket the value reported by Moorhead et al. (2003) of 257 g C m⁻² from organic matter cover on sediments and soils adjacent to Parera Pond, on the south side of Taylor Valley. In general, our results are within previously reported estimates of lake benthic mats at the high end, and lower mat biomass on the margins of small meltwater ponds and ephemeral streams in Taylor Valley.

Pigments

Chlorophyll-a was detected in all samples and comparable to concentrations present in MCM LTER chlorophyll-a data from several streams over 20 years in Taylor Valley (Kohler et al. 2015). While sites in the Canada Glacier ASPA had the most consistently high chlorophyll-a content and the greatest NDVI values, the McKnight Creek plot had the overall highest concentration of chlorophyll-a on average, 24.44 μ g g⁻¹ (Fig. 4a). McKnight Creek



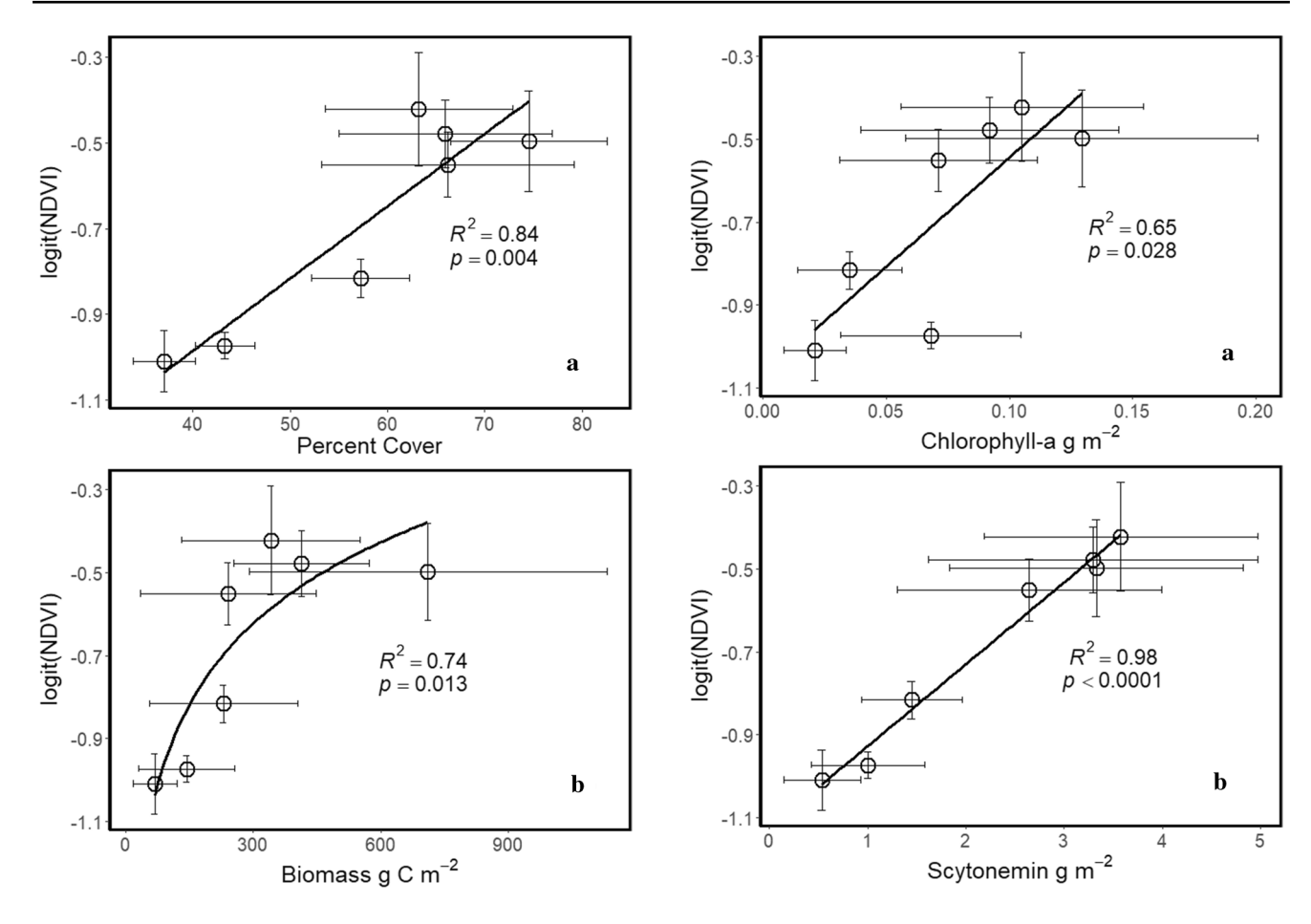


Fig. 6 Significant linear relationship between percent cover and logit(NDVI) (R^2 =0.84, p=0.004, logit(NDVI)=0.0169×cover-1. 66) (**a**). Significant logarithmic relationship between plot-scale biomass in g C m⁻² and logit(NDVI) (R^2 =0.74, p=0.013, logit(NDV I)=0.283×ln(biomass)-2.24) (**b**). Error bars indicate population standard deviation

Fig. 7 Significant linear relationship between plot-scale chlorophylla and logit(NDVI) (R^2 =0.65, p=0.028, logit(NDVI)=5.26×chlorophyll-1.07) (**a**). Highly significant linear relationship between plot-scale scytonemin and logit(NDVI) (R^2 =0.98, p<0.0001, logit(NDVI)=0.197×scytonemin-1.12) (**b**). Error bars indicate population standard deviation

samples also exhibited the most variation in chlorophyll-a concentrations (Fig. 4a), among the lowest percent cover of microbial mats and thus, on an areal basis, significantly lower chlorophyll-a mass than the Canada Stream sites (Tables 2 and 3). It is notable that although microbial mats at McKnight Creek occur at lower percent cover and biomass, they have autotrophic indices (i.e., Chl-a:AFDM) greater than those at Canada Stream (i.e., 0.32 compared to 0.15 average for the flush). Based on these results and noting that McKnight Creek has less stable substrate consisting of sand rather than cobble observed at the other sites, there is likely a higher turnover of microbial biomass due to shearing stress at McKnight Creek. It is possible that these are younger microbial mats in comparison to the mats sampled at Canada Stream and Green Creek, where the plots were in a more stable environment close to the source glacier with consistent but low flow and with low potential for shearing of microbial mats.

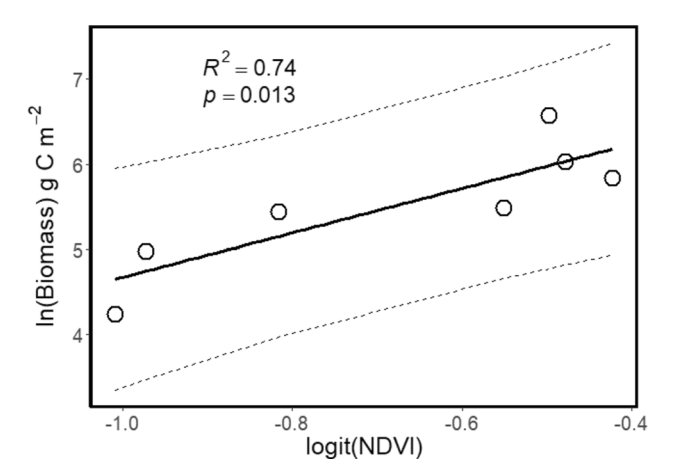


Fig. 8 Significant linear relationship between logit(NDVI) and the natural logarithm of plot-scale biomass in g C m⁻² (R^2 =0.74, p=0.013, ln(biomass)=2.61×logit(NDVI)+7.28). Dotted lines represent 95% prediction intervals. This is the relationship used to extrapolate biomass



Our pigment analysis also indicates high concentration of scytonemin in microbial mat samples, with the Canada Glacier lower flush area (i.e., Canada Stream 1-4) having the highest concentrations (ANOVA, df = 6, F = 5.04, p = 0.0003) (Fig. 4b). Average scytonemin concentrations for the Canada Glacier lower flush sites ranged from $495-700 \mu g g^{-1}$, or $400-566 \mu g cm^{-2}$, and are in the same range as values reported by Vincent et al. (1993), approximately 425 µg cm⁻² for black microbial mats sampled at the delta of Canada Stream. Because these plots are located adjacent to the Canada Glacier in a wetland area where they are less likely to scour, the microbial mats occurring here appear to be active and stable with multiple years of biomass accumulation. The other plots are in areas of more consistent channelized stream flow, where the microbial mats may be younger with less time to have accumulated biomass and pigments. While scytonemin is primarily produced under high UV, other environmental stressors (e.g., desiccation) have also been shown to increase scytonemin production (Fleming and Castenholz 2007). Further work on the perennial nature of these microbial mat ecosystems in stable wetland environments could shed light on the importance of scytonemin and other "sunscreen" pigments to the spectral dynamics of these environments and their importance to energy balance, UV protection, and C budgets.

Scaling ground-based observations to orbital spectral data

The average NDVI values for the Canada Stream lower flush area (i.e., Canada Stream 1-4) were all above 0.2 and were the highest NDVI values detected in our study (Fig. 5). NDVI averages for Green Creek and McKnight Creek were below 0.1 (Fig. 5). In traditional remote sensing applications, an NDVI value of 0.1 or lower is typically interpreted as unproductive ground, barren rock, or sand for example, and NDVI values between 0.2 and 0.5 are considered low biomass vegetation (e.g., shrub and steppe vegetation). However, the detection of low-density, patchy microbial mats is not anticipated to be comparable to typical uses of NDVI vegetation detection of macro-vegetation, e.g., trees, crops, etc. Although the NDVI averages for Green Creek and McKnight Creek were just below 0.1, we are confident that the spectral signatures are in fact detecting microbial mat presence at these sites. Locations in the regions surrounding the study areas that we knew were unvegetated, based on our field observations, had even lower NDVI values of 0.06-0.07. Similarly, Fretwell et al. (2011) determined pixels on the Antarctic Peninsula with NDVI values between 0.1 and 0.2 are considered "very probable" to have vegetation (i.e., a mean of 87.3% of pixels were within vegetated areas), and pixels between 0.05 and 0.1 are "probably vegetated" (i.e., 50–72% of pixels were within vegetated areas).

It is of note though, that NDVI values are relative to the image scene, and spectral properties of substrate determine NDVI detection. While we can compare our NDVI values to Fretwell et al. (2011), the substrate of the Fryxell Basin is different from the sites on the Antarctic Peninsula in that study, and therefore our actual detection limits are likely different. Since this is the first study to confirm microbial mat detection in the McMurdo Dry Valleys via NDVI combined with biological ground surveying, we don't have limits of vegetation detection in the MDV to compare our values to. Based on our observations, 0.09 was used as the conservative threshold for vegetation detection in this analysis, which corresponds to the lowest NDVI average detected in the Green Creek plot where low, but significant, biomass of microbial mats was found, and where previous studies have reported active and diverse microbial mat communities (Alger et al. 1997; Esposito et al. 2006; Stanish et al. 2011; Kohler 2015).

Percent cover and microbial mat biomass were both significantly correlated with logit(NDVI) (Fig. 6), notably higher than the correlation between chlorophyll-a and logit(NDVI) (Fig. 7a), which suggests that the NDVI signature is driven more by biomass and ground cover than chlorophyll activity. This is supported by the strong linear correlation of scytonemin with logit(NDVI) $(R^2 = 0.98,$ p < 0.0001) (Fig. 7b). NDVI is versatile, designed to broadly detect a variety of photosynthetic species. The darkening at visible wavelengths by scytonemin is equally, if not more, detectable in the NDVI parameter as the absorption of chlorophyll-a. These results (i.e., scytonemin has a stronger correlation with logit(NDVI) than chlorophyll-a does) appear to demonstrate how scytonemin is shielding underlying chlorophyll-a. While scytonemin is a sheath pigment and not involved in C fixation, its darkening at visible wavelengths and its strong reflection at NIR wavelengths was the most detectable signal in the spectral data and could be a useful indicator of perennial microbial mat biomass in satellite imagery.

These results demonstrate the utility and limitations of this method for examining cyanobacterial mat abundance in the MDV. For example, the strong correlations of NDVI with percent cover, biomass, and scytonemin demonstrate that WV-2 imagery is highly effective at detecting and estimating the biomass of dense perennial microbial mat communities. However, the weaker correlation between chlorophyll-a and NDVI, driven by the anomalously high chlorophyll-a concentrations but low NDVI signals at McKnight Creek, point to the difficulty of using NDVI to characterize productivity for microbial mat communities with patchy cover and/or low biomass. The microbial mat communities at McKnight Creek are noticeably different from the other sites we examined in this study (i.e., low organic matter in combination with high chlorophyll-a), likely due to differences in



substrate stability and possibly the longevity of microbial mats. Additionally, the stronger correlation with scytonemin than with any other variable suggests that additional investigation of the spectral properties of these communities may inform new approaches for characterizing the distribution of vegetation than traditional NDVI approaches. Although NDVI does not necessarily require chlorophyll-a correlations to detect biomass, shown here by the strong correlation between scytonemin, there are other "red-edge" approaches that might be more effective at detecting microbial mat *activity* through stronger chlorophyll-a correlations (Zhu et al. 2017).

Using normalized difference vegetation index to estimate microbial mat carbon inventories

Soils represent the vast majority of the McMurdo Dry Valley landscape; in Taylor Valley, for example, soils occupy 105 km², followed by lakes (4.7 km²), and streams (0.2 km²) (Burkins et al. 2001). The majority of Taylor Valley soils do not typically have visible surface mats or organic matter accumulations. For example, microbial mats and moss beds are found within and near streams and lakes; however, soils host fully functioning food webs and ecosystem processes even in some of the most arid environments (Adams et al. 2006; Barrett et al. 2006b; Lee et al. 2019). The majority of the organic C in Taylor Valley soils was thought to have originated from sediments deposited by previous high stands of pro-glacial lakes (Burkins et al. 2000). Burkins et al. (2001) estimated Taylor Valley lakes have on average 1250 g C m⁻², streams have a maximum of 600 g C m⁻², and soils have 150 g C m⁻², representing approximately 27%, 0.5%, and up to 72% of the total organic C in Taylor Valley when scaled to total ground cover, respectively. Our plot level averages for C content are comparable to stream C inventories from Burkins et al. (2001) with Green Creek representing the lower end at 69 g C m⁻² and the Canada Glacier lower flush plots representing the higher end at 242–711 g C m⁻².

Extrapolating from our carbon biomass model (Fig. 8), we estimated 21,715 kg of microbial mat C (95% prediction interval of 6312 to 74,871 kg of C) in the Canada Glacier ASPA in January 2018 (Fig. 2). This prediction brackets the estimation by Salvatore et al. (in review) of 35,804.3 kg of C in the Canada Glacier ASPA in December of 2018, using orbital data and handheld hyperspectral measurements. We estimate an average of 139 g C m⁻² for vegetated areas (i.e., pixels > 0.09 NDVI), which is surprisingly low compared to the values reported by Burkins et al. (2001) (i.e., 600 g C m⁻² for streams and 150 g C m⁻² for soils), since the ASPA is considered one of the most biologically active sites in Taylor Valley. However, even given the conspicuous, dense, and biological diverse mats of areas like the flush, arid soils make up the majority of the ASPA area, and these areas

are not included in previous studies of stream mats, organic matter, or C inventories (Schwarz et al. 1992; Alger et al. 1997); they are included in our C estimates. For comparison, in the Green Creek and Bowles Creek wetland area (Fig. 1), we estimated an average microbial mat biomass of 131 g C m^{-2} for vegetated areas (i.e., pixels > 0.09 NDVI) and for the lower reach of McKnight Creek, we estimated 114 g C m⁻² for vegetated areas. Our extrapolations of these biomass estimates at the low end of NDVI observations is intended to illustrate the potential importance of sparse microbial mat over broad spatial areas to regional C budgets and biological inventories. These results should be interpreted cautiously as NDVI values on the low end of these regression models are likely near the limits of biotic detection from satellites. Additionally, because we targeted unsubmerged plot areas in an effort to avoid spectral signatures dominated by water, the extrapolation presented here may likely underestimate biomass as a considerable amount of organic matter thrives under water. In ongoing work, we are using ground-based spectral measurements to verify the strong correlations reported here with higher resolution measurements and more intensive observations over greater spatial and temporal breadth, and importantly including areas with both inconspicuous mat cover and NDVI values near our 0.09 cutoff.

This study is the first in this region of Antarctica to estimate microbial mat biomass by quantitatively comparing biological surface observations to NDVI using satellite imagery. Such inventories are important to address ongoing questions about the sources and budgets of C in this region as well as to inform future management and policy decisions within the Antarctic Treaty Framework (Priscu and Howkins 2016). Our work suggests that while stream riparian and glacial wetland microbial mat communities are certainly hotspots of organic matter and biodiversity, as reported by others (Schwarz et al. 1992; Geyer et al. 2013, 2014, 2017), satellite imagery is also capable of detecting significant stocks of organic matter outside of stream channels and other biological hotspots. While our results don't significantly change previous C inventory estimates, they do point to ways in which improving the low end of NDVI detection could open up estimates of C in low-flow, or no-flow environments not previously considered in earlier studies. Indeed, our NDVI-derived biomass estimates suggest that low productivity environments, due to their broad spatial extents, may have more C overall than the highly productive areas in the Canada Stream ASPA and other riparian environments. This remote sensing application for detecting and estimating microbial mat abundance and activity, once validated, could be scaled to provide inventories of terrestrial C pools for the Lake Fryxell Basin, Taylor Valley, and potentially the entirety of the McMurdo Dry Valleys. Our continuing research (e.g., Salvatore et al. in review) is working towards the creation and validation of a remote



sensing tool that will allow us to systematically estimate the distribution and activity of terrestrial microbial mats in the MDV. Future work will aim to relate climatic events (e.g., high flow events) from the past (using archived satellite imagery) to determine how microbial mats respond to inter-annual climate variation and also potentially forecast how these primary producers may be affected in the future by a changing climate.

Acknowledgements The authors gratefully acknowledge Helen J. Peat and two anonymous reviewers whose feedback improved this manuscript. This project was supported by the National Science Foundation through Grant #1637708 to the McMurdo Dry Valleys Long Term Ecological Research Project and Grant #1745053 to M. Salvatore, Barrett, Sokol, and Stanish. We acknowledge the Polar Geospatial Center for geospatial support, DigitalGlobe, Inc. for access to satellite imagery, and UNAVCO of Boulder, CO, for assistance with high-resolution GPS. We also appreciate the logistical and helicopter contractors, Antarctic Support Contractors and Petroleum Helicopters Inc., for providing operational support in the field. We'd also like to thank Bobbie Niederlehner for her assistance with pigment analysis.

Data Availability The datasets generated and analyzed during this study are freely available from the HYPERLINK "http://mcm.lternet.edu/content/microbial-mat-biomass-and-normalized-difference-vegetation-index-ndvi-values-lake-fryxell" MCM LTER website as well as the HYPERLINK "https://portal.edirepository.org/nis/mapbrowse?scope=knb-lter-mcm&identifier=263&revision=1" Environmental Data Initiative Repository.

Compliance with Ethical Standards

Permission to enter the Canada Glacier Antarctic Specially Protected Area (ASPA 131) and sample microbial mat was given by the National Science Foundation Division of Polar Programs through Antarctic Conservation Act Permit ACA 2016-018. The authors declare no competing interests.

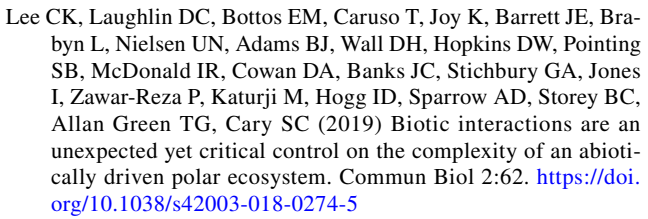
References

- Abed RMM, Al Kharusi S, Schramm A, Robinson MD (2010) Bacterial diversity, pigments and nitrogen fixation of biological desert crusts from the Sultanate of Oman. FEMS Microbiol Ecol 72:418–428. https://doi.org/10.1111/j.1574-6941.2010.00854.x
- Adams BJ, Bardgett RD, Ayres E, Wall DH, Aislabie J, Bamforth S, Bargagli R, Cary C, Cavacini P, Connell L, Convey P, Fell JW, Frati F, Hogg ID, Newsham KK, O'Donnell A, Russell N, Seppelt RD, Stevens MI (2006) Diversity and distribution of Victoria Land biota. Soil Biol Biochem 38:3003–3018. https://doi. org/10.1016/J.SOILBIO.2006.04.030
- Alger AS, McKnight DM, Spalding SA, Tate CM, Shupe GH, Welch KA, Edwards R, Andrews ED, House HR (1997) Ecological processes in a cold desert ecosystem: the abundance and species distribution of algal mats in glacial meltwater streams in Taylor Valley, Antarctica. Occasional Paper 51, University of Colorado Boulder, USA
- Andréfouët S, Payri C, Hochberg EJ, Che LM, Atkinson MJ (2003) Airborne hyperspectral detection of microbial mat pigmentation in Rangiroa atoll (French Polynesia). Limnol Oceanogr 48:426–430. https://doi.org/10.4319/lo.2003.48.1_part_2.0426

- Ayres E, Wall DH, Adams BJ, Barrett JE, Virginia RA (2007) Unique similarity of faunal communities across aquatic–terrestrial interfaces in a polar desert ecosystem. Ecosystems 10:523–535. https://doi.org/10.1007/s10021-007-9035-x
- Ball BA, Virginia RA, Barrett JE, Parsons AN, Wall DH (2009) Interactions between physical and biotic factors influence CO₂ flux in Antarctic dry valley soils. Soil Biol Biochem 41:1510–1517. https://doi.org/10.1016/J.SOILBIO.2009.04.011
- Barrett JE, Gooseff MN, Takacs-Vesbach C (2009) Spatial variation in soil active-layer geochemistry across hydrologic margins in polar desert ecosystems. Hydrol Earth Syst Sci Discuss 6:3725–3751. https://doi.org/10.5194/hessd-6-3725-2009
- Barrett JE, Virginia RA, Hopkins DW, Aislabie J, Bargagli R, Bockheim JG, Campbell IB, Lyons WB, Moorhead DL, Nkem JN, Sletten RS, Steltzer H, Wall DH, Wallenstein MD (2006a) Terrestrial ecosystem processes of Victoria Land, Antarctica. Soil Biol Biochem 38:3019–3034. https://doi.org/10.1016/J.SOILB IO.2006.04.041
- Barrett JE, Virginia RA, Wall DH, Cary SC, Adams BJ, Hacker AL, Aislabie JM (2006b) Co-variation in soil biodiversity and biogeochemistry in northern and southern Victoria Land. Antarctica Antarct Sci 18:535. https://doi.org/10.1017/S0954102006000587
- Barrett JE, Virginia RA, Wall DH, Parsons AN, Burkins MB (2004) Variation in biogeochemistry and soil biodiversity across spatial scales in a polar desert ecosystem. Ecol 85:3105–3118. https://doi.org/10.1890/03-0213
- Belnap J (2003) The world at your feet: desert biological soil crusts. Front Ecol Environ 1:181–189. https://doi.org/10.1890/1540-9295(2003)001[0181:TWAYFD12.0.CO:2
- Berner LT, Jantz P, Tape KD, Goetz SJ (2018) Tundra plant above-ground biomass and shrub dominance mapped across the North Slope of Alaska. Environ Res Lett 13:035002. https://doi.org/10.1088/1748-9326/aaaa9a
- Bollard-Breen B, Brooks JD, Jones MRL, Robertson J, Betschart S, Kung O, Craig Cary S, Lee CK, Pointing SB (2015) Application of an unmanned aerial vehicle in spatial mapping of terrestrial biology and human disturbance in the McMurdo Dry Valleys, East Antarctica. Polar Biol 38:573–578. https://doi.org/10.1007/ s00300-014-1586-7
- Burkins MB, Virginia RA, Chamberlain CP, Wall DH (2000) Origin and distribution of soil organic matter in Taylor Valley, Antarctica. Ecol 81:2377–2391. https://doi.org/10.1890/0012-9658(2000)081[2377:OADOSO]2.0.CO;2
- Burkins MB, Virginia RA, Wall DH (2001) Organic carbon cycling in Taylor Valley, Antarctica: quantifying soil reservoirs and soil respiration. Glob Chang Biol 7:113–125. https://doi.org/10.1046/j.1365-2486.2001.00393.x
- Collins W (1978) Remote sensing of crop type and maturity. Photogramm Eng Remote Sens 44:43–55
- Conovitz PA, Mcknight DM, Macdonald LH, Fountain AG, House HR (1998) Hydrologic Processes influencing streamflow variation in Fryxell Basin, Antarctica. In: Priscu J (ed) Ecosystem dynamics in a polar desert: the McMurdo Dry Valleys, Antarctica. American Geophysical Union, Washington D.C., pp 93–108
- Dodds WK, Gudder DA, Mollenhauer D (1995) The ecology of nostoc. J Phycol 31:2–18. https://doi.org/10.1111/j.0022-3646.1995.00002.x
- Doran PT, McKay CP, Clow GD, Dana GL, Fountain AG, Nylen T, Lyons WB (2002) Valley floor climate observations from the McMurdo dry valleys, Antarctica, 1986–2000. J Geophys Res 107:4772. https://doi.org/10.1029/2001JD002045
- Edwards R, Treitz P (2017) Vegetation greening trends at two sites in the Canadian Arctic: 1984–2015. Arctic, Antarct Alp Res 49:601– 619. https://doi.org/10.1657/AAAR0016-075
- Elbert W, Weber B, Burrows S, Steinkamp J, Büdel B, Andreae MO, Pöschl U (2012) Contribution of cryptogamic covers to the global



- cycles of carbon and nitrogen. Nat Geosci 5:459–462. https://doi.org/10.1038/ngeo1486
- Esposito RMM, Horn SL, McKnight DM, Cox MJ, Grant MC, Spaulding SA, Doran PT, Cozzetto KD (2006) Antarctic climate cooling and response of diatoms in glacial meltwater streams. Geophys Res Lett 33:L07406. https://doi.org/10.1029/2006GL025903
- Fleming ED, Castenholz RW (2007) Effects of periodic desiccation on the synthesis of the UV-screening compound, scytonemin, in cyanobacteria. Environ Microbiol 9:1448–1455. https://doi.org/10.1111/j.1462-2920.2007.01261.x
- Fountain AG, Nylen TH, Monaghan A, Basagic HJ, Bromwich D (2010) Snow in the McMurdo Dry Valleys, Antarctica. Int J Climatol 30:633–642. https://doi.org/10.1002/joc.1933
- Fretwell PT, Convey P, Fleming AH, Peat HJ, Hughes KA (2011) Detecting and mapping vegetation distribution on the Antarctic Peninsula from remote sensing data. Polar Biol 34:273–281. https://doi.org/10.1007/s00300-010-0880-2
- Garcia-Pichel F, Sherry ND, Castenholz RW (1992) Evidence for an ultraviolet sunscreen role of the extracellular pigment scytonemin in the terrestrial cyanobacterium Chlorogloeopsis sp. Photochem Photobiol 56:17–23
- Garcia-Pichel F, Castenholz RW (1991) Characterization and biological implications of scytonemin, a cyanobacterial sheath pigment. J Phycol 27:395–409. https://doi.org/10.1111/j.0022-3646.1991.00395.x
- Geyer KM, Altrichter AE, Takacs-Vesbach CD, Van Horn DJ, Gooseff MN, Barrett JE (2014) Bacterial community composition of divergent soil habitats in a polar desert. FEMS Microbiol Ecol 89:490–494. https://doi.org/10.1111/1574-6941.12306
- Geyer KM, Altrichter AE, Van Horn DJ, Takacs-Vesbach CD, Gooseff MN, Barrett JE (2013) Environmental controls over bacterial communities in polar desert soils. Ecosphere 4:1–17. https://doi.org/10.1890/ES13-00048.1
- Geyer KM, Takacs-Vesbach CD, Gooseff MN, Barrett JE (2017) Primary productivity as a control over soil microbial diversity along environmental gradients in a polar desert ecosystem. PeerJ 5:e3377. https://doi.org/10.7717/peerj.3377
- Gooseff MN, Mcknight DM, Doran P, Fountain AG, Lyons WB (2011) Hydrological connectivity of the landscape of the McMurdo Dry Valleys, Antarctica. Geogr Compass 5:666–681. https://doi.org/ 10.1111/j.1749-8198.2011.00445.x
- Hawes I, Sumner DY, Andersen DT, Jungblut AD, Mackey TJ (2013) Timescales of growth response of microbial mats to environmental change in an ice-covered antarctic lake. Biology (Basel) 2:151–176. https://doi.org/10.3390/biology2010151
- Hogrefe K, Patil V, Ruthrauff D, Meixell B, Budde M, Hupp J, Ward D (2017) Normalized difference vegetation index as an estimator for abundance and quality of avian herbivore forage in Arctic Alaska. Remote Sens 9:1234. https://doi.org/10.3390/rs9121234
- Jawak SD, Luis AJ, Fretwell PT, Convey P, Durairajan UA (2019) Semiautomated detection and mapping of vegetation distribution in the antarctic environment using spatial-spectral characteristics of WorldView-2 imagery. Remote Sens 11:1909. https://doi. org/10.3390/rs11161909
- Karnieli A, Kidron GJ, Glaesser C, Ben-Dor E (1999) Spectral Characteristics of cyanobacteria soil crust in semiarid environments. Remote Sens Environ 69:67–75. https://doi.org/10.1016/S0034-4257(98)00110-2
- Kohler TJ (2015) Physical and chemical controls on the abundance and composition of stream microbial mats from the McMurdo Dry Valleys, Antarctica. Dissertation, University of Colorado Boulder
- Kohler TJ, Stanish LF, Crisp SW, Koch JC, Liptzin D, Baeseman JL, McKnight DM (2015) Life in the main channel: long-term hydrologic control of microbial mat abundance in McMurdo Dry Valley Streams, Antarctica. Ecosystems 18:310–327. https://doi.org/10.1007/s10021-014-9829-6



- Levy J (2013) How big are the McMurdo Dry Valleys? Estimating ice-free area using Landsat image data. Antarct Sci 25:119–120. https://doi.org/10.1017/S0954102012000727
- Levy J, Cary SC, Joy K, Lee CK (2020) Detection and community-level identification of microbial mats in the McMurdo Dry Valleys using drone-based hyperspectral reflectance imaging. Antarct Sci. https://doi.org/10.1017/S0954102020000243
- McKnight DM, Niyogi DK, Alger AS, Bomblies A, Conovitz PA, Tate CM (1999) Dry valley streams in Antarctica: ecosystems waiting for water. Bioscience 49:985–995. https://doi.org/10.1525/bisi.1999.49.12.985
- Mcknight DM, Tate CM, Andrews ED, Niyogi DK, Cozzetto K, Welch K, Lyons WB, Capone DG (2007) Reactivation of a cryptobiotic stream ecosystem in the McMurdo Dry Valleys, Antarctica: a long-term geomorphological experiment. Geomorphology 89:186–204. https://doi.org/10.1016/j.geomorph.2006.07.025
- Miranda V, Pina P, Heleno S, Vieira G, Mora C, E.G.R. Schaefer C, (2020) Monitoring recent changes of vegetation in Fildes Peninsula (King George Island, Antarctica) through satellite imagery guided by UAV surveys. Sci Total Environ 704:135295. https:// doi.org/10.1016/j.scitotenv.2019.135295
- Moorhead DL, Barrett JE, Virginia RA, Wall DH, Porazinska D (2003) Organic matter and soil biota of upland wetlands in Taylor Valley, Antarctica. Polar Biol 26:567–576. https://doi.org/10.1007/s0030 0-003-0524-x
- Mulla DJ (2013) Twenty five years of remote sensing in precision agriculture: Key advances and remaining knowledge gaps. Biosyst Eng 114:358–371. https://doi.org/10.1016/J.BIOSYSTEMS ENG.2012.08.009
- Power SN, Salvatore MR, Sokol ER, Stanish LF, Barrett JE (2020) McMurdo Dry Valleys LTER: Microbial mat biomass and Normalized Difference Vegetation Index (NDVI) values from Lake Fryxell Basin, Antarctica, January 2018. Environmental Data Initiative. https://doi.org/10.6073/pasta/9acbbde9abc1e013f8c9fd9c383327f4
- Prieto-Barajas CM, Valencia-Cantero E, Santoyo G (2018) Microbial mat ecosystems: Structure types, functional diversity, and biotechnological application. Electron J Biotechnol 31:48–56. https://doi. org/10.1016/J.EJBT.2017.11.001
- Priscu JC, Howkins A (2016) Environmental assessment of the McMurdo Dry Valleys: witness to the past and guide to the future. Special publication, LRES-PRG 02, Montana State University, USA
- R Core Team (2017) R: A language and environment for statistical computing. R Foundation for Statistical Computing, Vienna, Austria. http://www.R-project.org
- Rodríguez-Caballero E, Paul M, Tamm A, Caesar J, Büdel B, Escribano P, Hill J, Weber B (2017) Biomass assessment of microbial surface communities by means of hyperspectral remote sensing data. Sci Total Environ 586:1287–1297. https://doi.org/10.1016/J. SCITOTENV.2017.02.141
- Salvatore MR (2015) High-resolution compositional remote sensing of the Transantarctic Mountains: application to the WorldView-2 dataset. Antarct Sci 27:473–491. https://doi.org/10.1017/S0954 10201500019X
- Salvatore MR, Borges SR, Barrett JE, Sokol ER, Stanish LF, Power SN, Morin P (2020) Remote characterization of photosynthetic



- communities in the Fryxell basin of Taylor Valley. Antarctica Antarct Sci. https://doi.org/10.1017/S0954102020000176
- Salvatore MR, Borges SR, Barrett JE, Power SN, Stanish LF, Sokol ER (in review) Counting carbon: quantifying biomass in the McMurdo Dry Valleys through Orbital & Field Observations. Sci Rep.
- Salvatore MR, Mustard JF, Head JW, Marchant DR, Wyatt MB (2014) Characterization of spectral and geochemical variability within the Ferrar Dolerite of the McMurdo Dry Valleys, Antarctica: weathering, alteration, and magmatic processes. Antarct Sci 26:49–68, https://doi.org/10.1017/S0954102013000254
- Schwarz AMJ, Green TGA, Seppelt RD (1992) Terrestrial vegetation at Canada Glacier, Southern Victoria Land, Antarctica. Polar Biol 12:397–404. https://doi.org/10.1007/BF00243110
- Stanish LF, Nemergut DR, McKnight DM (2011) Hydrologic processes influence diatom community composition in Dry Valley streams. J North Am Benthol Soc 30:1057–1073. https://doi.org/10.1899/11-008.1
- Treonis A, Wall D, Virginia R (1999) Invertebrate biodiversity in Antarctic Dry Valley soils and sediments. Ecosystems 2:482–492
- Tucker CJ (1979) Red and photographic infrared linear combinations for monitoring vegetation. Remote Sens Environ 8:127–150
- Vincent WF, Downes MT, Castenholz RW, Howard-Williams AC (1993) Community structure and pigment organisation of cyanobacteria-dominated microbial mats in Antarctica. Eur J Phycol 28:213–221

- Vincent WF, Howard-Williams C (1986) Antarctic stream ecosystems: physiological ecology of a blue-green algal epilithon. Freshw Biol 16:219–233. https://doi.org/10.1111/j.1365-2427.1986.tb00966.x
- Vítek P, Jehlička J, Ascaso C, Mašek V, Gómez-Silva B, Olivares H, Wierzchos J (2014) Distribution of scytonemin in endolithic microbial communities from halite crusts in the hyperarid zone of the Atacama Desert, Chile. FEMS Microbiol Ecol 90:351–366. https://doi.org/10.1111/1574-6941.12387
- Warton DI, Hui FKC (2011) The arcsine is asinine: the analysis of proportions in ecology. Ecology 92:3–10. https://doi.org/10.1890/10-0340.1
- Wetzel RG (1983) Limnology, 2nd edn. Saunders, Philadelphia
- Xue J, Su B (2017) Significant remote sensing vegetation indices: a review of developments and applications. J Sensors 2017:1–17. https://doi.org/10.1155/2017/1353691
- Zhu Y, Liu K, Liu L, Myint S, Wang S, Liu H, He Z (2017) Exploring the potential of WorldView-2 red-edge band-based vegetation indices for estimation of mangrove leaf area index with machine learning algorithms. Remote Sens 9:1060. https://doi.org/10.3390/rs9101060

Publisher's Note Springer Nature remains neutral with regard to jurisdictional claims in published maps and institutional affiliations.

